The Science and Technology of Slags for Iron and Steelmaking

A. McLean*, Y.D.Yang*, I.D. Sommerville*, Y.Uchida** and M.Iwase**

* *Department of Metallurgy and Materials Science, University of Toronto, Toronto, Canada,*
** *Department of Energy Science and Technology, Kyoto University, Kyoto, Japan*

(Received November 2, 2000)

ABSTRACT

In the quest to generate information pertaining to the characterization, properties and performance of molten slags, measurements and models are two interdependent requirements. Without measurements, our models are incomplete and unsatisfactory. Without models, we fail to realize, or perhaps even comprehend, the potential significance of our measurements. In this context, the concept of optical basicity will be revisited and examples presented of how optical basicity can be used to design slags with appropriate characteristics for specific applications in iron and steelmaking.

INTRODUCTION

In the quest to generate information pertaining to the characterization, properties and performance of molten slags, measurements and models are two interdependent requirements. Without measurements, our models are incomplete and unsatisfactory. Without models, we fail to realize, or perhaps even comprehend, the potential significance of our measurements.

In this context, the ratio of basic oxides to acidic oxides expressed in weight percent, or sometimes as a molar ratio, is traditionally used as a measure of slag basicity. However the simple (CaO/SiO_2) ratio ignores the effects of other oxides and the ratio ($CaO + MgO)/(Al_2O_3 + SiO_2$) implies that lime and magnesia behave as equivalent basic oxides and that alumina and silica have the same degree of acidity, neither of which is the case. To some degree, this can be offset by the use of empirical coefficients, although the modified ratios are somewhat restricted in their applicability to specific applications.

Optical basicity is a relatively new concept which provides a good foundation for a better understanding of the behaviour of molten slags than the conventional basicity ratios. The concept of optical basicity was developed by glass scientists /1/ and introduced to the metallurgical community by Duffy, Ingram and Sommerville in the late seventies /2/. This approach has proved to be a valuable tool for designing slags or fluxes which will have the required characteristics with respect to the behaviour of, for example, sulphur, phosphorus, hydrogen, magnesia and alkalis /3-8/. Optical basicity of molten slag can be calculated using the following relationships:

$$\Lambda = \sum_{i=1}^{n} \Lambda_i N_i \tag{1}$$

$$N_i = \frac{X_i n_{O_i}}{\sum_{i=1}^{n} X_i n_{O_i}} \tag{2}$$

Here Λ : Optical basicity of the slag
Λ_i : Optical basicity value of component "i"
N_i : Compositional fraction
X_i : Mole fraction of component "i" in the slag
n_{Oi} : Number of oxygen atoms in component "i"

In this paper the concept of optical basicity will be revisited and examples presented of how optical basicity

can be used to characterize the behaviour of oxide melts and to design slags with appropriate properties for specific applications in iron and steelmaking.

Measurement of Oxidation-Reduction Equilibria in Oxide Melts

In molten slags many transition metal cations can exist in two valency states and the red-ox equilibrium can be interpreted, at least conceptually, in terms of interaction between ions of different species and the extent of polymerization of the melt. For many years, it has been considered /9/ that the oxidation-reduction equilibrium for the Fe^{2+}/Fe^{3+}couple in glasses and slags could be expressed by either of the following reactions:

$$Fe^{2+} + \frac{1}{4}O_2 = Fe^{3+} + \frac{1}{2}O^{2-} \quad (3)$$

$$K(3) = \frac{(Fe^{3+})\,a_{O^{2-}}^{\frac{1}{2}}}{(Fe^{2+})\,P_{O_2}^{\frac{1}{4}}} \quad (4)$$

or

$$Fe^{2+} + \frac{1}{4}O_2 + \frac{3}{2}O^{2-} = FeO_2^- \quad (5)$$

$$K(5) = \frac{(Fe^{3+})}{(Fe^{2+})\,P_{O_2}^{\frac{1}{4}}\,a_{O^{2-}}^{\frac{3}{2}}} \quad (6)$$

where (Fe^{2+}) and (Fe^{3+}) are the concentrations of Fe^{2+} and Fe^{3+}, respectively, in pct by weight, and $a_{O^{2-}}$ is the activity of the oxygen anion. Conventional wet chemical analysis does not distinguish between FeO_2^- and Fe^{3+}, hence in Equation (6), the concentration of the tri-valent iron is expressed by (Fe^{3+}) rather than (FeO_2^-). Equations (3) and (5) are for acidic and relatively basic melts, respectively. It follows from Equations (4) and (6), that:

$$\log\left\{\frac{(Fe^{3+})}{(Fe^{2+})\,P_{O_2}^{\frac{1}{4}}}\right\} = -\frac{1}{2}\log a_{O^{2-}} + \log K(3) \quad (7)$$

and

$$\log\left\{\frac{(Fe^{3+})}{(Fe^{2+})\,P_{O_2}^{\frac{1}{4}}}\right\} = +\frac{3}{2}\log a_{O^{2-}} + \log K(5) \quad (8)$$

Although the absolute values of *K(3)* and *K(5)* are not measurable, a schematic representation corresponding to Equations (7) and (8) can be constructed as shown in Figure 1. For acidic melts, $\{(Fe^{3+})/(Fe^{2+})P_{O_2}^{1/4}\}$ should decrease with an increase in basicity or oxygen anion activity (Region I of Figure 1), while the reverse should hold true for relatively basic melts (Region II of Figure 1). Thus, the ratio $\{(Fe^{3+})/(Fe^{2+})P_{O_2}^{1/4}\}$ should exhibit a minimum turning point when plotted against basicity. This behavior is a reflection of the amphoteric character of ferric oxide. Based on these considerations, it is evident that the red-ox ratio is a qualitative indicator of slag basicity.

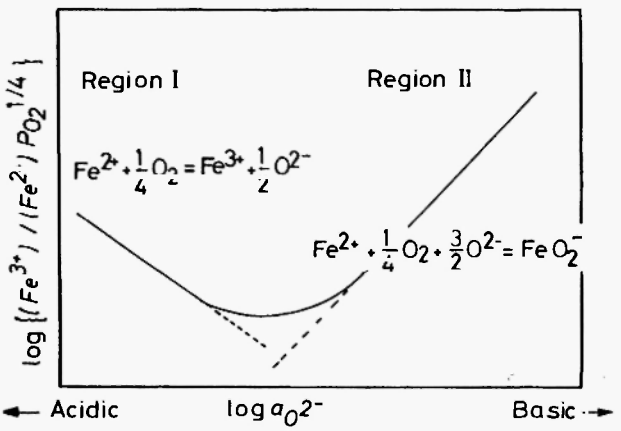

Fig. 1: Schematic diagram showing the relationship between the red-ox ratio and melt basicity at a fixed temperature /10/.

In order to demonstrate experimentally this anticipated variation of $\{(Fe^{3+})/(Fe^{2+})P_{O_2}^{1/4}\}$ with melt basicity, Ohashi *et al.* /10/ conducted oxidation-reduction equilibrium experiments with twenty-one oxide melts containing CaO, Li_2O, Al_2O_3, ZnO, B_2O_3, SiO_2 and small concentrations of iron oxide corresponding to total iron concentrations of about 1 to 4 wt%. The main oxide components can be classified as basic (CaO, Li_2O), amphoteric (ZnO, Al_2O_3) and acidic (SiO_2 , B_2O_3). If plotted on a schematic basic-acidic-amphoteric ternary composition diagram, then the melt compositions are represented by points A through U in Figure 2.

As shown in Table I, the Li_2O content of the melts decreases progressively from A through F, while the

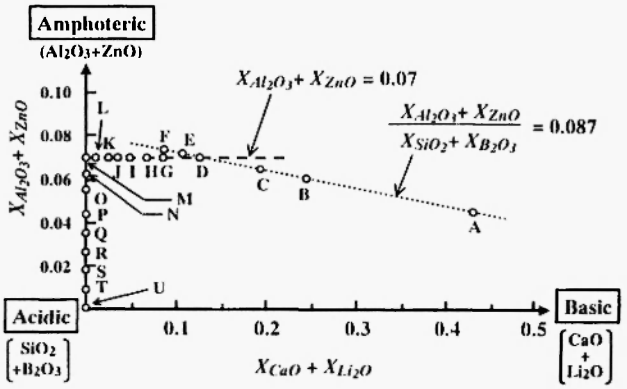

Fig. 2: Compositions of oxide melts A through U plotted on a Basic-Acidic-Amphoteric schematic ternary diagram /10/.

relative amounts of the other oxides are held constant, so that qualitatively the basicities should decrease in the same direction. The dotted line in Figure 2 corresponds to a constant ratio of {amphoteric oxides/acidic oxides} of 0.087. Points A through F are located along this line.

For melts G, H and I, the concentrations of silica, alumina, zinc oxide and lime were held constant while the sum of the mole fractions of lithium oxide and boron oxide was maintained at 0.25. The horizontal broken line in Figure 2 corresponds to a fixed concentration for the amphoteric oxides, alumina and zinc oxide of 0.07. Points G, H and I which lie on this line refer to melts with decreasing concentrations of Li_2O and therefore increasing concentrations of B_2O_3 . Consequently, the basicities of melts G, H and I, should decrease in this same order.

With oxide melts J, K, L and M, the lithium oxide content was zero and the concentrations of silica, alumina and zinc oxide remained constant at the same levels as those present in melts G, H and I. In this case however, the sum of the mole fractions of calcium oxide and boron oxide was maintained constant at 0.294. Since the concentrations of the amphoteric oxides (Al_2O_3 and ZnO) remain unchanged, points J, K, L and M also lie on the horizontal broken line. These points correspond to decreasing concentrations of CaO and therefore increasing concentrations of B_2O_3 Consequently, the basicities of J, K, L and M, decrease in this order.

For melts N through U, the concentration of silica remained constant at the same level as that present in melts G through M. However since these melts contain neither lime nor lithium oxide, points N through U are located on the acidic-amphoteric edge in Figure 2. In these melts the ratio $X_{Al_2O_3}/X_{ZnO}$ was kept essentially constant, while B_2O_3 progressively replaced ($X_{Al_2O_3}$ + X_{ZnO}) until the amphoteric content reached zero at point U. As the amphoteric oxides are replaced by acidic oxide, the basicity character decreases in the order N through U.

Thus from a qualitative standpoint, the basicities of the melts decrease progressively in the order A through U. As shown in Table I, this is represented quantitatively by a corresponding decrease in the optical basicity values for the glass melts. These values were calculated by Ohashi *et al.* /10/ using the following data reported by Duffy /11/ for the optical basicity of Li_2O and B_2O_3, and by Young *et al.* /6/ for the optical basicity of CaO, ZnO, Al_2O_3, and SiO_2:

CaO, 1.0; Li_2O, 1.0; ZnO, 0.95; Al_2O_3, 0.60; SiO_2, 0.46; B_2O_3, 0.42.

The results obtained from the oxidation-reduction equilibrium experiments for $\{(Fe^{3+})/(Fe^{2+})\ P_{O_2}^{1/4}\}$ when plotted against the optical basicity of the glass melts, Figure 3, are in accord with the schematic representation shown in Figure 1. The red-ox ratio first decreases with increasing optical basicity (Region I),

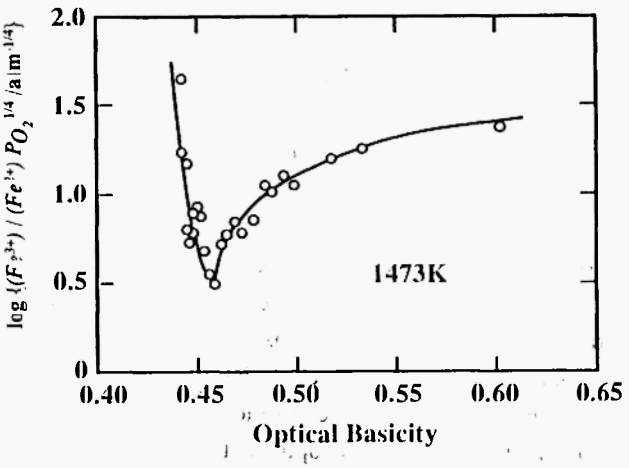

Fig. 3: Relationship between the red-ox ratio and optical basicity at 1473 K for oxide melts A through U /10/.

Table 1
Compositions of the melts investigated by Ohashi *et al.*/10/

Sample code	Melt composition						Optical Basicity
	X_{SiO_2}	$X_{B_2O_3}$	X_{Li_2O}	X_{CaO}	$X_{Al_2O_3}$	X_{ZnO}	
A	0.416	0.109	0.400	0.029	0.026	0.020	0.602
B	0.554	0.146	0.200	0.038	0.035	0.026	0.532
C	0.589	0.155	0.150	0.041	0.037	0.028	0.518
D	0.636	0.167	0.082	0.044	0.040	0.030	0.499
E	0.651	0.172	0.060	0.045	0.041	0.031	0.493
F	0.665	0.176	0.040	0.046	0.042	0.031	0.488
G	0.636	0.209	0.041	0.044	0.040	0.030	0.485
H	0.636	0.230	0.021	0.044	0.040	0.030	0.478
I	0.636	0.250	0	0.044	0.040	0.030	0.471
J	0.636	0.261	0	0.033	0.040	0.030	0.468
K	0.636	0.272	0	0.022	0.040	0.030	0.465
L	0.636	0.283	0	0.011	0.040	0.030	0.462
M	0.636	0.294	0	0	0.040	0.030	0.458
N	0.636	0.303	0	0	0.035	0.026	0.456
O	0.636	0.312	0	0	0.030	0.022	0.454
P	0.636	0.320	0	0	0.025	0.019	0.452
Q	0.636	0.329	0	0	0.020	0.015	0.450
R	0.636	0.338	0	0	0.015	0.011	0.448
S	0.636	0.346	0	0	0.010	0.008	0.446
T	0.636	0.355	0	0	0.005	0.004	0.444
U	0.636	0.364	0	0	0.000	0.000	0.442

passes through a minimum and then increases with further increase in optical basicity (Region II). Transition from Region I to Region II occurs at an optical basicity value of about 0.46. In view of the major differences in chemical composition in these complex multi-component oxide melts, the red-ox behaviour cannot be represented in terms of a basicity ratio. The fact that the red-ox behaviour, within both acidic and basic regimes, could be represented in terms of optical basicity provides further support for effective implementation of the optical basicity model with respect to the characterization and design of slags for industrial applications. These aspects are discussed in the following sections.

OPTICAL BASICITY APPLICATIONS IN BLAST FURNACE OPERATIONS

The formation of volatile species associated with sodium and potassium have adverse effects on blast furnace operation due to refractory attack, generation of fines, accretion formation and decreased burden permeability. Problems of this type are accentuated when furnaces operate with higher driving rates, increased flame temperatures, lower slag volumes and higher basicities. Problems associated with alkalis can be alleviated by decreasing the alkali input to the furnace or by adjusting the slag composition and operating parameters. However, raw material with a low

alkali content is not always available and therefore alkali control by careful design of slag chemistry is an important consideration with respect to the resolution of alkali problems. Lower slag basicity and lower flame temperatures will favour alkali accumulation in the slag phase. However, these adjustments may result in higher sulphur hot metal and lower productivity.

The opposing tendencies for alkali and sulphur removal in the blast furnace are generally considered in terms of the CaO/SiO_2 ratio as the measure of slag basicity. For many years, such an assumption was adequate; however, advances in blast furnace practice have presented additional complexity with respect to the expression of slag basicity. These advances include improvement in slag fluidity, reduced hot metal silicon content and extension of the refractory hearth life and are associated with higher levels of magnesia, alumina and titanium oxide respectively.

The dissolution of potassium oxide in blast furnace slag under equilibrium conditions has been measured by Karsrud /12/. The results obtained for slags with a CaO/SiO_2 ratio between 0.9 and 1.3 are given in Figure 4. As shown in this figure, the potassium oxide content of the slag decreases with increasing CaO/SiO_2 ratio. Figure 4 also shows that for slags with a constant CaO/SiO_2 ratio, the alkali concentrations decrease with increasing magnesia content /8/.

However, Figure 5 suggests the opposite conclusion, i.e. that a slag rich in magnesia should be able to hold more alkali. This apparent contradiction can be rationalized by comparing Figures 4 and 5. In Figure 4, the CaO/SiO_2 ratio is used to measure the slag basicity, whereas in Figure 5 the slag basicity is expressed in terms of $(CaO+MgO)/SiO_2$. In Figure 4, an increase in magnesia content in a slag with a fixed CaO/SiO_2 ratio represents an increase in slag basicity, and consequently a decrease in alkali content. In Figure 5, an increase in magnesia content in a slag with a fixed $(CaO+MgO)/SiO_2$ ratio actually constitutes a decrease in slag basicity, since CaO, a strong basic oxide, is being replaced by MgO, a weaker basic oxide. Under these circumstances, an increase in magnesia yields a slag with a greater ability to absorb alkalis.

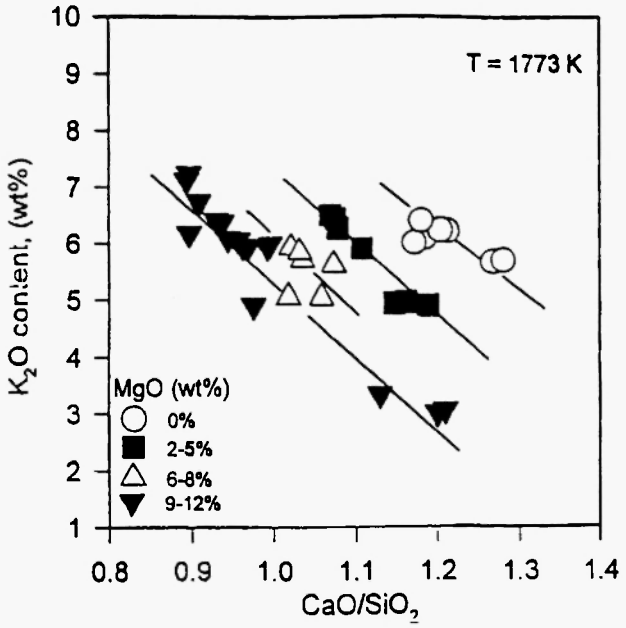

Fig. 4: Dependence of potassium oxide content on CaO/SiO_2 ratio and magnesia concentration of synthetic blast furnace slags, derived from experimental results of Karsrud /12/.

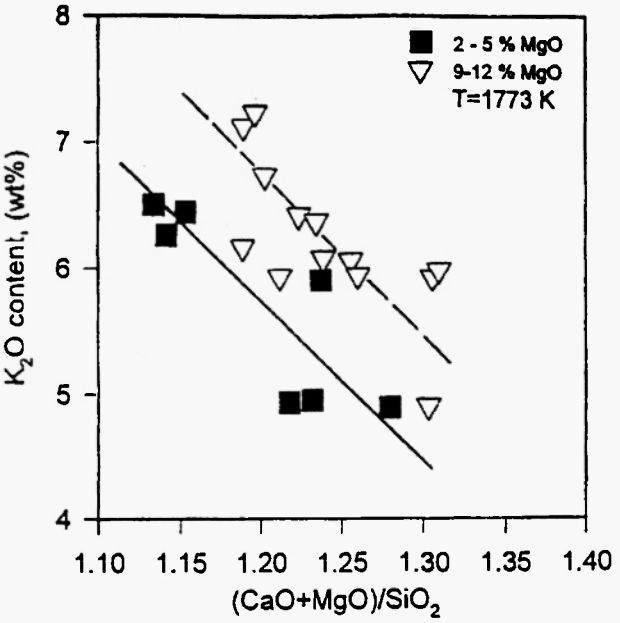

Fig. 5: Effect of magnesia concentration on potassium oxide content of synthetic blast furnace slags with $(CaO+MgO)/SiO_2$ ratio as a basicity index, Karsrud /12/.

The potential for confusion, and the possibility of reaching a wrong conclusion, with respect to the effect of magnesia on the alkali content of slag, or for that

matter other constituents such as sulphur or phosphorus, highlights the disadvantage of using variable, empirical ratios as indicators of slag basicity. Using experimental data reported by Karsrud /12/, Bergman, in 1989, was the first to propose a correlation between the solubility of potassium oxide in blast furnace slag and optical basicity /13/:

$$\log (\text{wt\% } K_2O) = -7.12\Lambda + 5.49 \quad (9)$$

Yang *et al.* /8/, have re-examined both laboratory results and plant data on alkalis, using the concept of optical basicity to characterize slag behaviour rather than conventional basicity ratios. From the experiments conducted by Karsrud /12/, Yang *et al.* calculated the K_2O capacity of the slag, defined as follows:

$$2K(g) + \tfrac{1}{2} O_2 = K_2O \text{ (slag)} \quad (10)$$

$$K(10) = \frac{a_{K_2O}}{P_K{}^2 \cdot P_{O_2}{}^{0.5}} \quad (11)$$

$$C_{K_2O} = \frac{(wt\%K_2O)}{P_K{}^2 \cdot P_{O_2}{}^{0.5}} = \frac{K(10)}{f_{K_2O}} \quad (12)$$

As shown in Figure 6, the alkali capacity decreases

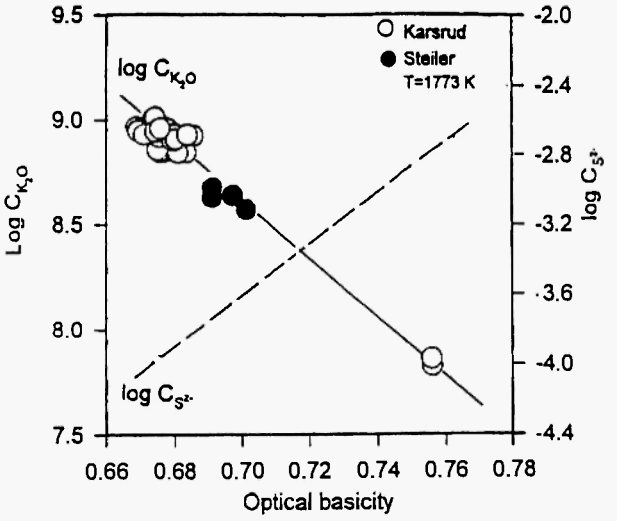

Fig. 6: Dependence of the potassium oxide capacity and sulphide capacity of molten slags on optical basicity (derived from results of Karsrud /12/ and Steiler /14/).

with increasing optical basicity /8/. The two data points with optical basicity values of about 0.76 show a very low alkali capacity. The compositions of the corresponding slags are about 50% CaO, 49% Al_2O_3 and a small amount of SiO_2. While it is clearly not appropriate to express these two results in terms of the CaO/SiO_2 ratio, and even though they do not represent blast furnace slag compositions, it is of benefit to include these data in the figure as a further demonstration of the usefulness of the optical basicity approach. Also included in Figure 6 are data calculated from the work of Steiler /14/. The basicities of these slags are slightly higher than those of normal blast furnace slags. However, as shown in this figure, all of the data are located on the same straight line, and the potassium oxide capacity decreases with increasing optical basicity of the slag phase. This behaviour can be represented by the following regression equation /8/ which is valid for a slag temperature of 1500°C (1773K):

$$\log C_{K_2O} = -13.34\Lambda + 17.94 \quad (r^2 = 0.95) \quad (13)$$

The range of applicability of this equation is greater than that corresponding to Equation (9), the derivation of which incorporated a narrower range of slag compositions.

Sulphur capacity or sulphur distribution data for different slag systems are often plotted against the lime-silica ratio. Under these circumstances, there is a separate line for each slag system. However when plotted against optical basicity, the data can be reasonably represented by a single line. From a quantitative evaluation of desulphurization data for a number of different slag systems, Sosinsky and Sommerville /4/ derived the following correlation between sulphide capacity and optical basicity, which is valid for a temperature of 1500°C (1773K):

$$\log C_{S^{2-}} = 12.60\Lambda - 12.30 \quad (r^2 = 0.97) \quad (14)$$

This correlation of sulphide capacity with optical basicity is shown by the broken line in Figure 6. As shown in this figure, the alkali capacity decreases, and sulphide capacity increases, with increasing optical basicity. Thus with the aid of the optical basicity model,

an optimum slag composition can be designed for different blast furnace operations in order to establish appropriate conditions in order to control the behaviour of alkalis as well as sulphur.

OPTICAL BASICITY APPLICATIONS IN STEELMAKING OPERATIONS

At the Third International Slag Conference, a paper was presented which described how the optical basicity model was incorporated into the process control scheme for the converter steelmaking operation at BHP Steel International Group, and as a consequence, a significant reduction in production costs was achieved /15/. There are also opportunities for the optical basicity approach to be applied in post-furnace operations. For example, the absorption of hydrogen by molten steel is strongly affected by the composition of the slag phase and this has important implications with respect to ladle slags as well as the selection of tundish fluxes and continuous casting mold powders.

At this point, tribute must be paid to the pioneering studies on water vapour dissolution in slags by J. Chipman, T.B. King and co-workers at M.I.T. /16/, M. Imai, H. Ooi and T. Emi at Kawasaki Steel Corporation /17/, and T. Fuwa and his research group at Tohoku University /18/ during the 1950's and 60's.

In a similar manner to that described for alkalis and sulphur, when the water vapour content of molten slags is plotted as a function of the basicity ratio, Figure 7, different lines are obtained for different slag systems /19/. In this case, however, the relationships are curvilinear rather than linear due to the amphoteric behaviour of water vapour in molten slags. In acidic slags, the water vapour content actually decreases with increasing basicity, while with basic slags the reverse is true. When the water vapour capacity is plotted against optical basicity, Figure 8, the curvilinear relationship is again observed, however all of the data for different slag systems can be represented by a single line. From a quantitative evaluation of water vapour data for a number of different slag systems, Yang *et al.* /7/, derived the following correlation which is valid for temperatures around 1500-1600 °C (1773-1873K):

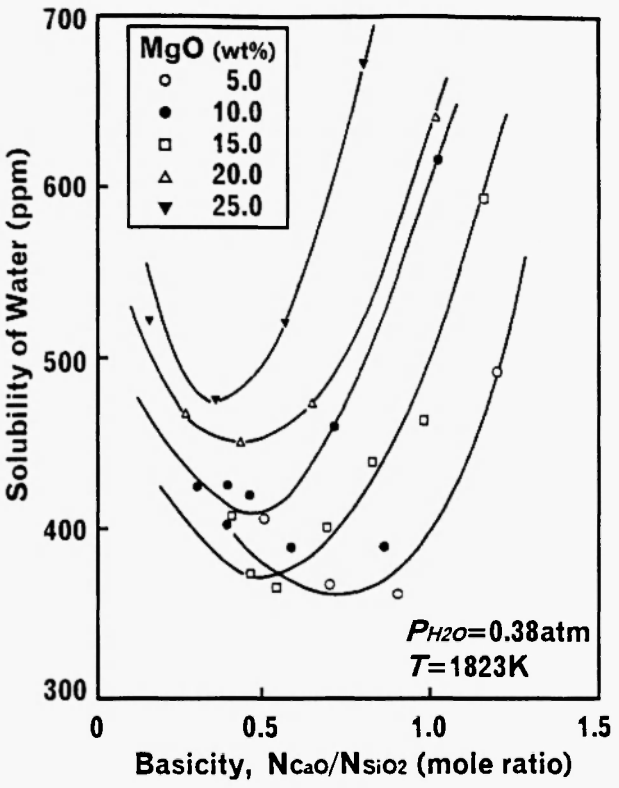

Fig. 7: Dependence of water vapour content on CaO/SiO_2 ratio and magnesia concentration of synthetic slags /19/.

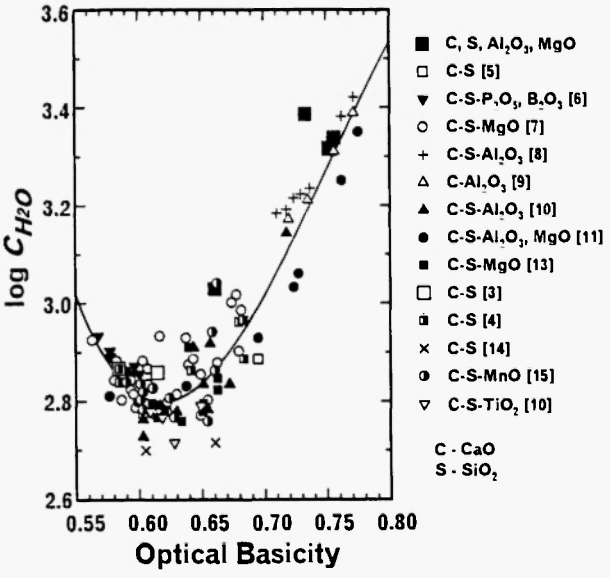

Fig. 8: Dependence of water vapour capacity of molten slags on optical basicity /7/
(The reference numbers correspond to those in the paper by Yang *et al.* /7/)

$$\log C_{H_2O} = 41.92 - 164.92\Lambda + 226.42\Lambda^2 - 100.31\Lambda^3 \quad (r^2 = 0.87) \qquad (15)$$

In acidic slags, $\Lambda<0.6$, water vapour reacts as a basic oxide and the water vapour capacity of the slags decreases with increasing slag basicity. In highly basic slags, $\Lambda>0.65$, water vapour reacts as an acidic oxide and water vapour capacity increases with increasing slag basicity. In slags with $\Lambda=0.6$ to 0.65, the water vapour capacity remains constant with increasing slag basicity, due to a mixture of basic and acidic reactions.

Since a high basicity slag will more readily absorb moisture from the atmosphere and transfer hydrogen into the steel than a low basicity slag, in order to minimize hydrogen pickup by the steel, a low basicity slag would be more effective than a high basicity slag. Unfortunately, these conditions, like those for alkali removal in the blast furnace, are the opposite of those that would be most appropriate for good sulphur removal. Thus for grades of steel which require strong desulphurization and where hydrogen pickup could be a problem, an optimum slag composition has to be selected taking into account these conflicting considerations. On the other hand, to minimize sulphur loss from the metal, for example during the production of high-sulphur machining grades, a slag with a lower optical basicity value would be appropriate which in addition, would be beneficial in minimizing hydrogen absorption by the steel.

CONCLUDING COMMENTS

At the beginning of a new century, with the availability of analytical facilities for the rapid and accurate determination of the chemical composition of metallurgical slags and synthetic fluxes, together with computational capabilities for the mathematical modeling of complex industrial systems, new control strategies can be designed in ways which were not possible when operating practices were first developed using empirical basicity ratios. In his 1987 Extractive Metallurgy Lecture, Professor Julian Szekely reviewed the state of mathematical modeling and its important role within extractive metallurgy /20/. In this excellent paper, he emphasized the fact that "Both process optimization and process control require a quantitative representation of the process." He also stressed the concept that "Calculations and measurements are not alternatives, but most often must be pursued in a complementary fashion." From the examples described in this paper, it will be evident that the optical basicity model provides an opportunity to design slag compositions for a broad range of specific functions, in a more precise and comprehensive manner, than would be the case with conventional basicity ratios. With this approach, improvements in both optimization and control of iron and steelmaking processes are achievable objectives. In his lecture, Professor Szekely went on to say, "The main barrier to the implementation of these concepts tends to be the non-availability of suitably trained personnel." Here then is the challenge for the future. In the final analysis, high quality products require high quality processing and both require high quality people. People will continue to constitute the critical link in order to promote communication and encourage collaborative partnerships which will not only enhance the two-way transfer of experience between the laboratory and the workplace but also facilitate the development and utilization of new knowledge.

REFERENCES

1. J.A. Duffy and M.D. Ingram, "Establishment of an Optical Scale for Lewis Basicity in Inorganic Oxyacids, Molten Salts and Glasses", *J. Am. Ceram. Soc.*, **93**, 6448-6454 (1971).
2. J.A. Duffy, M.D. Ingram and I.D. Sommerville, "Acid/Basic Properties of Molten Oxides and Metallurgical Slags", *J. Chem. Soc. Faraday Trans.*, **74** (6), 1410-1419 (1978).
3. T. Nakamura, Y. Ueda and J.M. Toguri, "A New Development of the Optical Basicity", *Trans. JIM*, **50**, 456-461 (1986).
4. D.J. Sosinsky and I.D. Sommerville, "The Composition and Temperature Dependence of the Sulphide Capacity of Metallurgical Slags", *Met. Trans. B*, **17B**, 331-337 (1986).
5. A. Bergman, "Some Aspects on MgO Solubility in

Complex Slags", *Steel Research*, **60** (5), 191-195 (1989).

6. R.W. Young, J.A. Duffy, G.J. Hassall and Z. Xu, "Use of Optical Basicity Concept for Determining Phosphorus and Sulphur Slag-Metal Partitions", *Ironmaking and Steelmaking*, **19** (3), 301-219 (1992).
7. Y.D. Yang, Z.A. Daya, I.D. Sommerville and A. McLean, "Water Vapour Solubility in Tundish Slags", *J. Iron & Steel Res. Int.*, **5** (2), 7-14 (1998), also *The Second International Conference on Continuous Casting of Steel*, The Chinese Society for Metals, Wuhan, China, 1997; pp.113-120.
8. Y.D. Yang, A. McLean, I.D. Sommerville and J.J. Poveromo, "The Correlation of Alkali Capacity with Optical Basicity of Blast Furnace Slags", *Iron & Steelmaker (Transactions)*, **27** (10), 103-111 (2000).
9. E.T. Turkdogan, *Physicochemical Properties of Molten Slags and Glasses*, The Metal Society, London, 1983.
10. S. Ohashi, M. Kashimura, Y. Uchida, A. McLean and M. Iwase, "Oxidation-Reduction Equilibria of Ferrous/Ferric Ions in Oxide Melts", *Steel Research*, **71** (10), 375-380 (2000).
11. J.A. Duffy, "Use of Refractivity Data for Obtaining Optical Basicities of Transition Metal Oxides", *Ironmaking and Steelmaking*, **19** (6), 426-28 (1989).
12. K. Karsrud, "Alkali Capacities of Synthetic Blast Furnace Slags at 1500°C", *Scandinavian Journal of Metallurgy*, **13**, 98-106 (1984).
13. A. Bergman, "A New Model on K_2O Solubility in Blast Furnace Slags", *Steel Research*, **60** (9), 383-386 (1989).
14. J.M. Steiler, "Study on Thermodynamics of Liquid K_2O-SiO_2 and K_2O-CaO-SiO_2-Al_2O_3-MgO Systems", *IRSID, Physico-Chimie et Siderurgie*, Versailles, France, Oct. 1978; pp. 254-257.
15. C.L. Carey, R.J. Serje, K. Gregory and H. Qinglin, "Optical Basicity: A Flexible Basis for Flux Control in Steelmaking", *3rd International Conference on Molten Slags and Fluxes*, The Institute of Metals, London, U.K., 1989; pp. 157-162.
16. J.H. Walsh, J. Chipman, T.B. King and N.J. Grant, "Hydrogen in Steelmaking Slags", *J. Metals*, **8**, 1574-1575 (1956).
17. M. Imai, H. Ooi and T. Emi, "On Dissolution of Water Vapour in Molten Slags", *Tetsu-to-Hagane* (in Japanese), **48**, 111-117 (1962).
18. T. Fukushima, Y. Iguchi, S. Ban-ya and T. Fuwa, "The Solubility of Water in Liquid Silicate", *Trans. ISIJ*, 6, 19-26 (1966).
19. Y. Iguchi and T. Fuwa, "The Solubility of Water in Liquid CaO-SiO_2-MgO, with and without "FeO" at 1550°C", *Trans. ISIJ*, **10**, 29-35 (1970).
20. J.Szekely, "The Mathematical Modeling Revolution in Extractive Metallurgy", *Met. Trans B*, **19B**, 525-540 (1988).